Cell–cell conjugation

Transient analysis and experimental implications

Aydin Tozeren
Department of Mechanical Engineering, The Catholic University of America, Washington, DC 20064 USA

ABSTRACT In the present study we investigate the transient conjugation of cell pairs by using a mathematical model. Macromolecules responsible for adhesion (bonds) are assumed to exist in two reversible states, attached and unattached, and exert a force elastic in nature only when they cross-link the two cell surfaces (attached state). Bonds form a link between the two cell surfaces only in the attached form. The unattached bridges are assumed laterally mobile in the plane of the cell membrane. Lateral mobility of attached bonds may be limited by structures on the undersurface of the cell membrane. Using this model we show that the bond density distribution between a cytotoxic T-cell (F-1) and a cancer cell (JY:HLA-A2-B7-DR4, W6) approaches equilibrium within 10 min, the incubation period used in experiments by Sung, K. L. P., L. A. Sung, M. Crimmins, S. J. Burakoff, and S. Chien (1986. *Science [Wash. DC]*. 234:1405–1408). If the diffusion coefficient of attached bonds is set equal to zero in the computations the model predictions indicate accumulation of bonds at the edge of conjugation. This prediction is consistent with present experimental data on lectin-induced red blood cell aggregation (Vayo, M., R. Skalak, P. Brunn, S. Usami, and S. Chien. 1987. *Fed. Proc.* 46:1043). It is concluded that significant features of micromanipulation data on specific adhesion can be explained by the diffusivity properties of bonds responsible for adhesion.

INTRODUCTION

Cell–cell adhesion induced by cross-linking macromolecules (bonds) plays a fundamental role in morphogenesis, intercellular recognition, blood rheology, and cell-mediated immunity. The relative strength of adhesion between various cell pairs can be quantified by in vitro experimental methods using radioactive cell binding essays (1–4). However, it is not yet possible to deduce the biophysical parameters of cross-linking macromolecules from such experimental data. The bond parameters of interest are: (*a*) their surface number density, (*b*) their elastic stiffness, (*c*) their diffusivity in attached and unattached configurations, (*d*) their binding affinity, and (*e*) the rates of transition between various biochemical states in the bond cycle.

Recently new in vitro methods have been introduced to quantify the adhesive energy density of conjugated cell pairs (5–11). Evans and his colleagues (5, 6) have introduced a micromanipulation technique to study cell–cell adhesion. In this technique, interaction of a pair of cells are studied under microscope. Each cell of the pair is held at the tip of a micropipette by suction, and the cells are brought together by manipulating the holding pipettes. After a period of incubation (transient conjugation) aspiration pressure holding one of the cells is increased stepwise and the pipette holding cell 1 is gradually pulled away (by micromanipulation). With sufficiently high aspiration pressures the two cells can be separated completely. The micromanipulation data consists of the measurements of aspiration pressures, the radii of the holding pipettes, the area (radius) of conjugation, the angles cells 1 and 2 make with the surface of contact at the edge of conjugation and the angles cells make with the radial direction at the tips of the pipettes. Using principles of static equilibrium, Evans and Leung (6) have derived a simple equation for the adhesive energy density γ (dynes per centimeter) in terms of the aforementioned parameters of micromanipulation data. γ is defined as the energy per unit area that must be supplied externally to separate conjugated cell pairs. γ is typically constant during adhesion and peeling of various adhesive tapes used in industry. However, it was found not to be constant during forced separation of lectin-induced red blood cell aggregates (6, 9) and during separation of a cytotoxic T-cell from its target cell (12). In Fig. 1 we present typical experimental data showing the strong dependence of γ on the extent of separation. This data indicates that γ is not an intrinsic parameter of adhesion but a function of evolving bond density distribution at the edge of conjugation. Hence, it is necessary to correlate the adhesive energy density γ deduced from experimental data to the biophysical parameters of adhesion.

Significant progress has been made in understanding the micromechanics of specific adhesion between cell pairs (Bell [13], Bell et al. [14], Bongrand et al. [15], and

0006-3495/90/09/641/12 $2.00

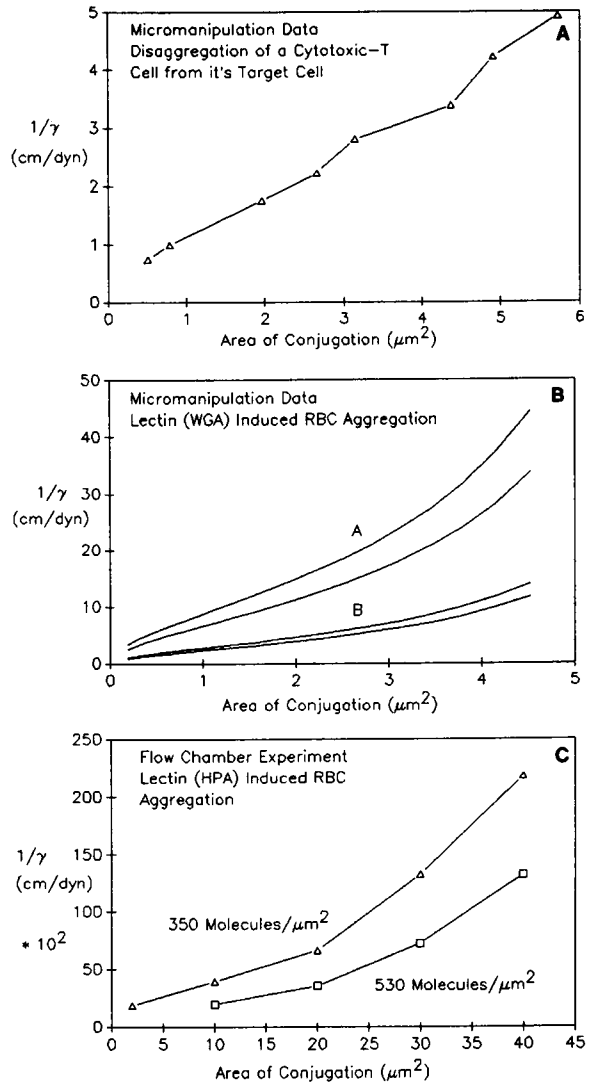

FIGURE 1 Typical experimental data on separation of conjugated cell pairs indicating the dependence of adhesive energy density γ on the extent of separation ([*A*] Tozeren et al. [18], [*B*] Evans and Leung [6], and [*C*] Chien and Sung [9]).

Dembo and Bell [16]). The model developed by Bell and colleagues was used to predict the contact area and the number of bonds between conjugated cell pairs after the process of adhesion reached equilibrium. More recently, Evans (7, 8) investigated the coupling between micromechanics of cell adhesion and the continuum equations of the adhering cell membranes. Evans (8) proposed that kinetically trapped bridges are responsible for the large peel tensions measured during the disaggregation of erythrocyte pairs which are bonded with wheat germ agglutinin. The same experimental data was also considered in a more recent study by Dembo et al. (17). In their model, adhesion is induced by bonds that are fixed in the plane of the membrane and the chemical reaction of bond formation and breakage is reversible. In numerical experiments on transient peeling, they showed that peeling resulting from application of a constant membrane tension comes to a halt when the detachment rate is assumed to decrease towards zero with increasing bond extension (catch bonds).

Immobile bond models of adhesion mentioned above may provide a reasonable approximation of events occurring during cell–cell adhesion if the lateral mobility of (attached and unattached) bonds are inhibited by the internal cell structure. Recent fluorescence data (McCloskey and Poo [7]) indicates that the bonds holding the cells together must be mobile. To deduce the biophysical parameters of mobile bridges (molecules responsible for adhesion) from experimental data we have introduced a model for the micromechanics of cell–cell adhesion (Tozeren et al. [18], Tozeren [19]). In the simplest case bonds exist in two reversal states, attached and unattached, and exert a force elastic in nature only when they cross-link the two cell surfaces (attached state). Both mutual and self diffusion of bonds are allowed. The self-diffusion coefficient is a measure of the random motion of an individual protein macromolecule and can be used to estimate an upperbound for the rate of bond formation between two cell surfaces (20, 21). Mutual diffusion refers to relaxation of gradients in macromolecule number density distribution. It is defined by Stokes-Einstein relation (21). In the present study, gradients in number densities of bonds are caused (*a*) by rapid formation of bridges in the region of conjugation and (*b*) the elastic energy stored in bridges by membrane tensions. In other biological phenomena, membrane protein concentration may vary with location on the cell surface in regions of coated pits where protein insertion depletion occurs (22) or in regions of developing axon (23). According to the fluid-mosaic model of Singer and Nicholson (24), most biological cell membranes act as two-dimensional (surface) fluids. However, the lateral mobility of the protein macromolecules may be restricted by peripheral structures such as tight junctions or cytoskeletal matrices. Our model takes into account these possible restrictions by assigning different diffusion coefficients for actual bonds linking the two cell surfaces (attached bonds) and receptor sites (unattached bonds).

One of the predictions of this model is that the number density of cross-linking macromolecules and their binding affinity can be determined from micromanipulaton data on critical tension that prevents further spread of conjugation. It is predicted that $1/\gamma$ is a linearly increasing function of the area of conjugation (A_c) for conjugation at biochemical and static equilibrium. This prediction is in excellent agreement with experimental data on the conjugation of a cytotoxic T-cell with its target cell (12). In this

case adhesion is induced by the binding of TCR, CD2, and LFA-1 molecules on the surface of a cytotoxic T-cell with molecules MHC II, LFA-3, and ICAMs on the surface of a target (cancer) cell (3). The micromanipulation data used in computations was obtained at an average peeling rate on the order of 0.004 μm/s. This rate is small but nonetheless finite. Another critical assumption that led to the linear variation of $1/\gamma$ with A_c was the assumption of uniform equilibrium distribution of bonds in the region of conjugation before the initiation of forced separation. In micromanipulation experiments, the incubation period was chosen as 10 min because the area of conjugation reached its maximum during this period. The duration of 10 min is short enough to avoid the occurrence of cytolysis during separation.

In the present paper, we study in detail the bond migration during transient conjugation (period of incubation) by constructing a set of numerical experiments with biophysically appropriate parameter values. This study is necessary to test the validity of the set of hypotheses that led to the aforementioned prediction and determine the time required to reach equilibrium during incubation. By curve fitting experimental data with transient analysis, indirect information on the bond diffusivity and their rates of attachment and detachment may be deduced. An investigation of cross-linking macromolecule events that occur during transient conjugation forms the first step of analysis of experimental data obtained during the subsequent forced separation.

In section 2 we present the equations governing bond migration during transient conjugation. In section 3 we introduce a set of dimensionless bond parameters that determines the micromechanics of cell–cell adhesion. We discuss the effects of these parameters on the time-variation of adhesive energy density and the number of attached bonds during the period of incubation in relation with existing literature. A bond model with multiple attached states is introduced in section 4. Results are summarized in the last section.

2.1 EQUATIONS GOVERNING BOND MIGRATION DURING CELL–CELL ADHESION

For simplicity in presentation, we consider a conjugated pair of identical membranes with uniform thickness and width as shown in Fig. 2. The coordinates x and y and the arc length s are defined in the same figure. The (x, y) coordinate system is attached to the edge of separation. Arc length s is zero at the origin and increases from left to right. The force-free length of an attached bond is arbitrarily set equal to the thickness of the adhering cell

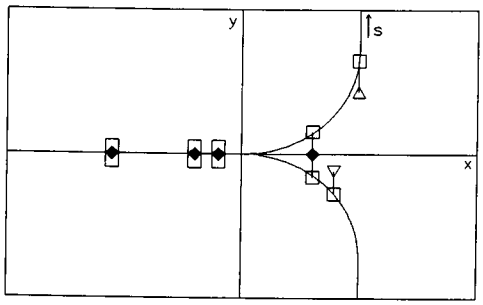

FIGURE 2 Schematic diagram of the edge of conjugation of a pair of cells linked by macromolecules (bonds).

membranes, so that the coordinate y represents the elastic extension in one of the two links of an attached bridge.

The bond number density n (1 per square nanometer) is defined as the number of attached bonds per unit surface area. Similarly m (1 per square nanometer) denotes the corresponding density for unattached bridges. In general m and n are functions of time t and arc length s. Next we define the flux density parameters J_m and J_n as the rates of bond transport per unit length:

$$J_m = m\,\langle V_m\rangle, \quad J_n = n\,\langle V_n\rangle, \tag{1}$$

where $\langle V_m\rangle$ and $\langle V_n\rangle$ denote, respectively, the average velocities of unattached and attached bridges in the direction of increasing s.

A bond flux can occur only in response to a force with two distinct types of forces assumed to contribute. The first is the elastic force in an attached bridge which pulls the bond towards the remaining area of conjugation reducing the strain in the attached configuration. The second type of force is the diffusional force that tends to restore a uniform number density for the bonds. In the case where the physical boundaries of the region of conjugation do not vary with time, J_m and J_n can be written as (Tozeren et al. [18]):

$$f_m J_m = k_b T_b\,(\partial m/\partial s) \tag{2a}$$

$$f_n J_n = k_b T_b\,(\partial n/\partial s) - n\,K\,y\,(\partial y/\partial s), \tag{2b}$$

where K (dynes per centimeter) denotes the bond stiffness, f_m and f_n are the drag coefficients for the lateral mobility, k_b denotes the Boltzman constant, and T_b is the absolute temperature. f_m and f_n characterize the resistance of the membrane to having bonds dragged through it. When the bond number density is low enough so that the bond–bond interaction can be neglected, diffusion coefficients D_{mm} and D_{nn} are related to the friction coefficients f_m, f_n as follows (25):

$$D_{mm} = k_b T_b/f_m; \quad D_{nn} = k_b T_b/f_n. \tag{3}$$

The basic free energy functions (A_m, A_n) of an unattached and an attached bond, respectively, are assumed to be

$$A_m = A_m^0 \tag{4a}$$

$$A_n = A_n^0 + \tfrac{1}{2} K(y)^2, \tag{4b}$$

where A_m^0 and A_n^0 are constants, and K is the bond stiffness constant (dynes per micrometer). A_m and A_n represent, respectively, the chemical potential of unattached and attached bonds at a standard bond number density (1 bond per square micrometer).

The time rate of attachment and detachment of bonds is assumed to be governed by the following set of rate equations:

$$\partial m/\partial t + \partial J_m/\partial s = g\,n - f\,m \tag{5a}$$

$$\partial n/\partial t + \partial J_n/\partial s = f\,m - g\,n, \tag{5b}$$

where f (seconds $^{-1}$) and g (seconds^{-1}) are the rates of attachment and detachment, respectively.

As shown in Bell's model of specific adhesion (13), bond formation is governed by a bimolecular reaction:

$$m + u \underset{g}{\overset{h}{\rightleftharpoons}} n,$$

where m denotes the number density of unattached receptors on cell No. 1, u is the number density of unattached receptors in cell No. 2, and n is the number density of attached bonds. The transient solutions involving bimolecular reactions are often quite complex (26). However, in two special cases the rate equations governing bimolecular bond formation involves only the number densities of attached and unattached bonds (m, n). In the first case, the number of receptors and coreceptors on cells 1 and 2 are approximately the same, and the surface areas of the conjugating cells are also comparable ($m = u$). Eq. 5 then represents the time course of bond formation provided that the attachment rate ($f\,m$) in this equation is replaced by $h\,m^2$. This modification is not expected to have a significant impact on the later stages of conjugation when bond migration takes place.

The kinetic Eq. 5 is a very good approximation of the bimolecular reaction of bond formation if the number density of coreceptors is much larger than that of receptors ($u \gg m$) so that u does not change significantly during the time course of cell–cell conjugation ($f = h\,u$). This special case is applicable to the formation of rosettes between human T lymphocytes and erythrocytes. In rosetting, receptors CD2 on T lymphocytes bind to coreceptors LFA-3 on erythrocytes. As measured by satura tion mAb binding, there are 10^5 and 4×10^3 CD2 and LFA-3 molecules on lymphocytes and erythrocytes, respectively (3). Hence the formation of attached bonds between a T lymphocyte and an erythrocyte will not change significantly the number density of free CD2 (u). CD2 and LFA-3 are known to contribute fundamentally to the adhesion between a cytotoxic T-cell and its target cell (3).

The rate functions f and g are not assigned arbitrarily, but are assumed to satisfy the condition of detailed balance, namely (27),

$$f/g = \exp\left([A_m^0 - A_n^0) - \tfrac{1}{2} K(y)^2\right]/k_b T_b). \tag{6}$$

In the present study we have assumed that the rate of detachment g increases with bond extension y such that

$$g = g_0 \exp\,[4y^2/(1 + y^2)], \tag{7}$$

where g_0 is the detachment rate at zero extension ($y = 0$). The attachment rate f is determined by combining Eqs. 6 and 7. According to Eq. 7, bond detachment rate increases asymptotically to a finite value with increasing bond extension. The assumption of an unbounded detachment rate ($g \to \infty$ as $y \to \infty$) was found to hamper the numerical computations. Fig. 3 shows the assumed variation of f and g with respect to bond extension y. There is no direct experimental justification for the form of Eq. 7. In general the rate parameters of an unstressed bond ($y = 0$) can be related to the biochemical rate constants of bonds measured in solution and to the surface self-diffusion coefficients of these bonds (Bell [13]). The role of the functional form of g on transient conjugation is investigated in the next section.

Eqs. 2 and 5, describing the micromechanics of cell–cell conjugation, are a set of quasilinear second order partial differential equations of parabolic type. The initial and boundary conditions must be specified before these equations can be solved. The boundary conditions at the center of the region of conjugation ($s = -z$) and at the free end $s = \ell$ are obtained by setting the fluxes of

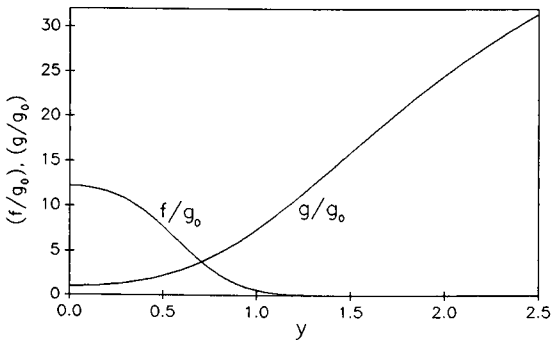

FIGURE 3 The rate functions f and g used in computations as a function of bond extension (Y). Binding affinity $b = \ln(f_0/g_0) = 2.5$, and the dimensionsless bond stiffness, $C = 10$.

attached and unattached bonds equal to zero at these two locations:

$$(\partial m/\partial s) = (\partial n/\partial s) = 0. \tag{8}$$

The boundary condition 8 is equivalent to the condition that the number of bridges on the cell surfaces remain constant during incubation. In the axisymmetric cell–cell conjugation, $s = -z$ corresponds to the center of the region of conjugation and $s = \ell$ then defines the other appex of the cell. If no bonds are assumed to be attached at time $t = 0$, the initial condition can be written as

$$n = 0,\ m = m_0 \text{ for } -z < s < \ell. \tag{9}$$

m_0 denotes the uniform bond number density before conjugation takes place.

The variation of bond extension (y) with respect to arc length (s) must be known in order to solve Eqs. 2 and 4. In the present study the angles the conjugated cells make with the plane of conjugation are assumed to be 90° (fig. 2). It can then be shown that the equations of equilibrium of a flexible membrane can be satisfied with the simple solution $(dy/ds) = 1$ outside a small region (edge of conjugation) where bridges are strained. At the edge of conjugation we assume that y increases from zero along a circular arc of radius r until (dy/ds) becomes equal to one (Fig. 2). In the computations r was taken equal to $(1/20) \times$ the radius of conjugation. A two-fold decrease in r resulted in a 2% change in the evaluated number of attached bonds. This ad hoc assumption of membrane curvature at the edge of conjugation is rather arbitrary but is necessitated by the already complex nature of Eqs. 2 and 4. The addition of two more parameters, namely membrane bending rigidity and membrane elasticity, would further complicate the interpretations of numerical computations. In our previous study of equilibrium bond density distribution, we have coupled Eqs. 2 and 4 to the equations of equilibrium of inextensible membranes (19, 20). In their adhesion models, Evans (8) and Dembo (17) considered the more realistic case of a membrane with finite bending rigidity. However, in these studies the parameters employed in analysis did not include the diffusion coefficients of bonds. The details of the numerical method of solution of Eqs. 2 and 4 are outlined in Appendix 2.

3.1 RESULTS

We will introduce a set of dimensionless variables and parameters in order to discuss our results. The dimensionless time T and dimensionless arc length S are defined as

$$T = g_0 t,\quad S = s/H, \tag{10}$$

where g_0 is the rate of detachment (seconds^{-1}) and H is a typical length. We take H to be equal to the length of the conjugation region divided by 100. H then becomes a reasonable upperbound for bond extension y.

Dimensionless density distributions M and N are defined as

$$M = m/m_0,\quad N = n/m_0, \tag{11}$$

where m_0 is the uniform bond density before conjugation and m and n are the densities of unattached and attached bonds, respectively, during transient conjugation. In the computations we evaluate N and M as a function of T and S throughout the incubation period.

Adhesive energy density γ is equal to twice the membrane tension T_0 measured at a distance from the edge of conjugation for the 90° peeling considered here. γ is computed as a function of dimensionless time T by using the equation (Tozeren et al. [18]):

$$\gamma = 2\int_0^y K\, y\, (dy/ds)\, n(s) ds. \tag{12}$$

At equilibrium, γ assumes the following value:

$$\gamma_{eq} = 2k_b T_b\, m_0\, N_{eq}, \tag{13}$$

where the subscripts eq are used to specify the corresponding equilibrium values. Note that $M_{eq} = 1/(1 + (f_0/g_0)(z/(\ell + z)))$, $N_{eq} = (f_0/g_0)M_{eq}$, where f_0, and g_0 denote, respectively, the rates of attachment and detachment of unstrained cross-bridge. The parameters N, M, and γ/γ eq are computed in terms of the bond diffusion coefficients D_{mm} and D_{nn}, bond stiffness K and the rate parameters f_0 and g_0. We group these constants into the following dimensionless parameters:

$$A = D_{mm}/(H^2 g_0),\quad b = \ell n\,(f_0/g_0)$$
$$C = KH^2/k_b T_b,\quad d = D_{nn}/D_{mm}. \tag{14}$$

The values $A = 10^3$, $b = 2.5$, and $C = 10$ were chosen for the control case. These are biophysically reasonable parameter values and fall within the range given by Bell et al. (14) and Dembo et al. (17). For example, $A = 10^3$ corresponds to $D_{mm} = 10^{-9}$ cm^2/s, $g_0 = 1$ s^{-1} and $H = 10$ nm. $C = 10$ corresponds to $H = 10$ nm, K = 0.41 dyn/cm, and $k_b T_b = 4.1 \times 10^{-14}$ dyn/cm (25°). In our computations we have considered two distinct values for d. In Model 1, we assumed that both the attached and unattached bonds are laterally mobile with identical diffusion coefficients, that is $D_{mm} = D_{nn}$, and hence $d = 1$. In model 2, we assumed that the lateral mobility of the attached bonds may be inhibited by internal structures so that $D_{nn} = 0$, hence $d = 0$.

Another parameter that is used in computations is the ratio of the total length of the membrane strip to the length of the region of conjugation. We denote this ratio

by parameter L. In the standard case L was assumed to be equal to 3.

3.1. Functional dependence of rate functions on bond extension

In our standard computations, we have used Eq. 7 to describe the strain dependence of rate of detachment (g). The rate of attachment (f) is then obtained by using Eqs. 6 and 7 (see Fig. 3). In this formulation, detachment rate increases with increasing bond extension (distortion), as in cross-bridge models of muscle contraction (26–29). Dembo et al. (17) calls this type of bond a slip-bond. They suggest that the rate of detachment of a highly stretched bond may actually be slower than the rate of detachment of an unstressed bond (catch-bonds). The stress created by stretching the bond acts as a lever to lock the bonding groups more tightly together. The detachment rate used by Dembo and colleagues in their Figs. 3 and 6 is written below in our notation:

$$g = g_0 \exp(-0.025CY^2), \qquad (15)$$

where Y is the dimensionless bond extension ($Y = y/H$) and f is determined by inserting Eq. 15 into Eq. 6. We have carried out a set of computations (model 2) using Eq. 15. The computed variation of adhesion energy density with respect to time during transient conjugation is shown for catch-bonds in Fig. 4. Also shown in the same figure γ/γ_{eq} vs. T curve corresponding to our control parameter values (slip-bonds). The figure shows that the model predictions on transient conjugation are not sensitive to the assumed functional form of the detachment rate but is sensitive to binding affinity (f/g). Recently, Dembo et al. (17) and Tozeren (19) have obtained similar results in their studies of adhesion induced by laterally

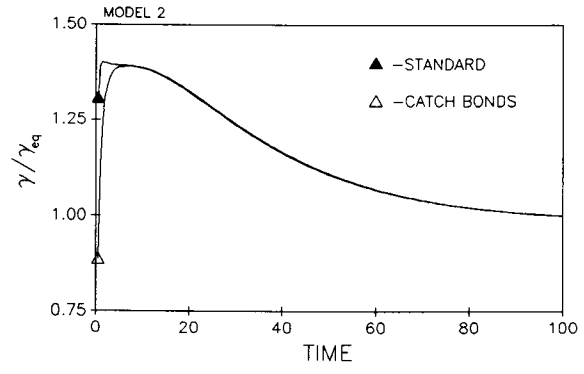

FIGURE 4 Adhesive energy density as a function of time during transient conjugation. Computations were performed using model 2 equations ($d = 0$) with g given by Eq. 7 for the standard curve (slip-bonds) and g given by Eq. 15 for catch-bonds.

fixed bridges. Dembo et al. (17) showed that the time course of annealing under constant membrane tension is not sensitive to the functional forms of f and g, but that the time course of peeling is completely transformed if the bonds are of catch-bond type ($g \to 0$ as $y \to \infty$). In this case the membrane will start to peel but will quickly come to a halt when the membrane tension is greater than the tension required to prevent further spreading of conjugation. In the computations presented below we have used only the rate functions given by Eqs. 6 and 7. Since our computations are restricted to transient conjugation, this is justified by the results shown in Fig. 4 as well as by earlier studies on immobile bonds (17, 19).

3.2 Effect of cell shape on transient conjugation

The equations of adhesion presented in section 2 are based on a two-dimensional geometry schematically shown in Fig. 2. The only independent space variable is the arc length along the membrane strip with constant unit width. This geometry has been used in previous models of cell–cell adhesion (7, 8, 17–19) as well as in other biophysical studies involving molecular aspects of force development. For example, in models of muscle contraction, axial displacement of a cross-bridge from the nearest action site is considered to be the only independent space variable (26–29). However, myosin cross-bridges protrude from the thick filaments of muscle fibers at regular intervals and therefore they are not mobile. The diffusion of mobile molecules on a three-dimensional surface may be significantly different than the one predicted by one-dimensional diffusion equations used in section 2. We have tested the consequences of the cell shape by numerically investigating conjugation of a spherical cell to a more flexible cell. This type of cell–cell interaction was first considered experimentally by Evans and Baxbaum (5). The equations governing bond migration along meridional directions on a spherical surface are given in Appendix 1. In our numerical computations we have considered the adhesion of a flexible cell to a spherical cell of radius $(4/\pi)$ μm. The area of conjugation was assumed in the form of a spherical cap with a maximum meridional angle of 45°. The longest meridional distance S_c along the arc length in the region of conjugation is then equal to 1 μm. We have taken the length parameter H as again 10 nm. Fig. 5 shows the bond number density distribution at various times during the period of incubation for cross-bridges cycling and migrating along a spherical surface. Also shown in Fig. 5 *B* the corresponding results obtained by using equations presented in section 2. In this figure we have chosen L to be equal to the ratio of the surface area of the spherical cell to the area of conjugation. This choice assures that both cases shown in the figure approach the

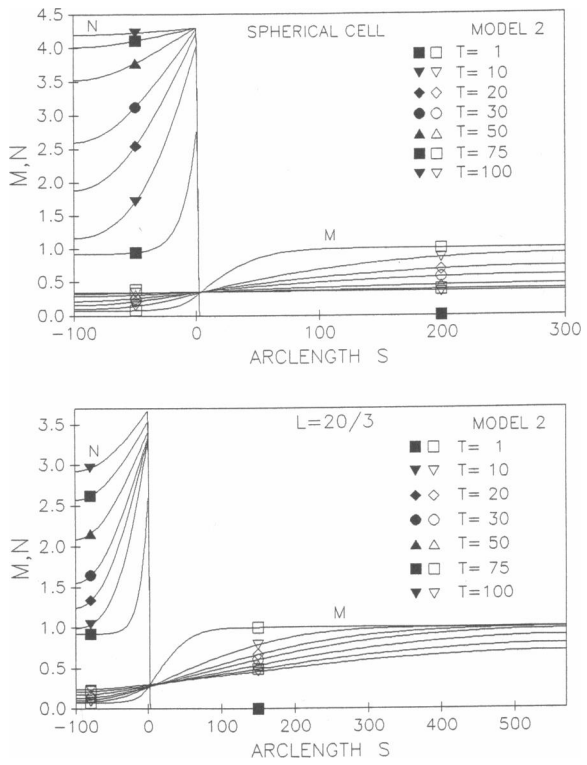

FIGURE 5 The density distribution of attached (N) and unattached (M) bonds on a spherical cell at various times (T) after the initiation of conjugation. The radius of the cell is $4/\pi$ μm. $A = 1{,}000$, $b = 2.5$, $C = 10$, $d = 0$ (model 2). The figure also shows the density distributions corresponding to the one-dimensional diffusion equations presented in section 2. Note that the arc length S is much longer in this case, however, N reaches the same equilibrium value in both graphs as $T \to \infty$.

same equilibrium bond density distributions. Fig. 5 shows that time required to reach equilibrium is shortened by at least fourfold for adhesion induced by bridges over a spherical surface. This is not surprising. The majority of unattached bridges are located close to the edge of conjugation along a spherical surface because of the intrinsic topology of the three-dimensional surface.

Our numerical results show that the shape and size of the cell have significant effects on the time required to reach equilibrium. The larger the size, the smaller will be the dimensionless parameter A. In fact, A is inversely proportional to the square of the radius of a spherical shell. Our numerical computations on spherical cells also show that the density distribution of bonds holding a cytotoxic T-cell (f1) and its target cell (JY) can be approximated reasonably well with equilibrium distribution after ~8 min of incubation. Bond parameters corresponding to this result are: $D_{mm} = 4 \times 10^{-9}$ cm^2/s, $D_{nn} = 0$, $K = 0.41$ dyn/cm, $b = 2.5$. The radius of the cytotoxic cell is modeled as $8/\pi$ μm. If the attached bonds are assumed mobile, the time to reach equilibrium will be shortened by at least twofold. This shows that 10-min incubation times used in experiments presented by Sung et al. allows for the bond density distribution to approach equilibrium.

3.3 Effect of bond diffusivity on transient conjugation

In our model, we allow different diffusion coefficients for attached and unattached bridges. The attached bridge diffusivity may be smaller than the corresponding diffusivity of unattached bridges because of its relatively larger size. This will be the case in ligand-induced adhesion. It is also expected that increased density of attached bridges will lead to lower values of bridge diffusivity. Finally there is the possibility that the attached bonds may be linked to internal structures of the cell such as actin gel in lymphocytes or membrane structures such as spectrin network in erythrocytes. To investigate the role of varying bond diffusivity we have carried out numerical experiments in which (a) $D_{mm} = D_{nn}$ (model 1) and (b) $D_{nn} = 0$ (model 2). The bond density distributions at various stages during transient conjugation are shown for these cases in Fig. 6. In model 1 bond density is reasonably uniform during the course of transient conjugation. If the mutual diffusivity of attached bonds are inhibited, the computations shown in Fig. 6 indicate that attached bonds accumulate at the edge of conjugation for long periods of time before equilibrium is reached.

The adhesive energy density γ gradually increases with time to the value reached at equilibrium for model 1 (Fig. 7). In the present computations the boundaries of the region of contact is kept constant. If one assumes that bond density distributions at the edge do not vary significantly at low speeds of annealing from the ones presented here, it is then expected that bond model 1 would correspond to a gradual increase in the area of conjugation during the period of incubation. This type of gradual spreading of conjugation is observed in the interaction of cytotoxic T-cells with their target cells (12). Fig. 7 *B* shows the time variation area of conjugation between a cytotoxic T-cell (F1) and its target cell (JY) measured by Sung et al. (12) (Fig. 1 in reference 12). Also shown in the figure is the (γ/γ_{eq}) vs. T curve for model 1. A more exact comparison of model predictions with data would require information on the time constants of the membrane unfolding process.

γ is slightly greater than the equilibrium value during the transient conjugation for model 2 (Fig. 8). Hence, the tendency of conjugation to spread is small. This predicted behavior is in agreement with data on erythrocyte aggregation induced by lectins (6, 11) but not with the afore-

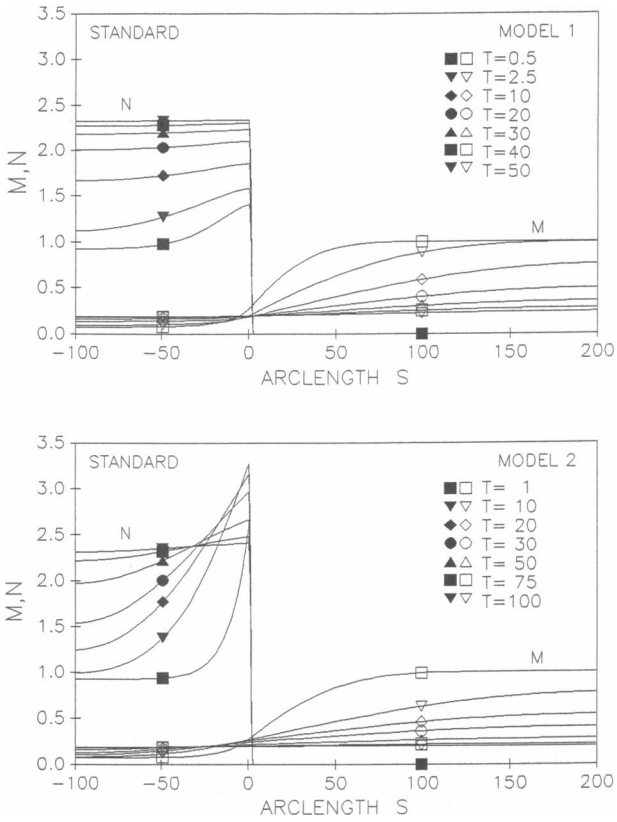

FIGURE 6 The density distribution of attached (N) and unattached bonds (M) at various times (T) after the initiation of conjugation. Fig. 6 *A* corresponds to model 1 in which the bonds are mobile in both attached and unattached configurations. Parameter values used in the computations are: $A = 1{,}000$, $b = 2.5$, $C = 10$, $d = 1$, and $L = 3$. *B* corresponds to model 2 in which the attached bonds are assumed immobile ($d = 0$). All other parameter values are the same as in Fig. 6 *A*.

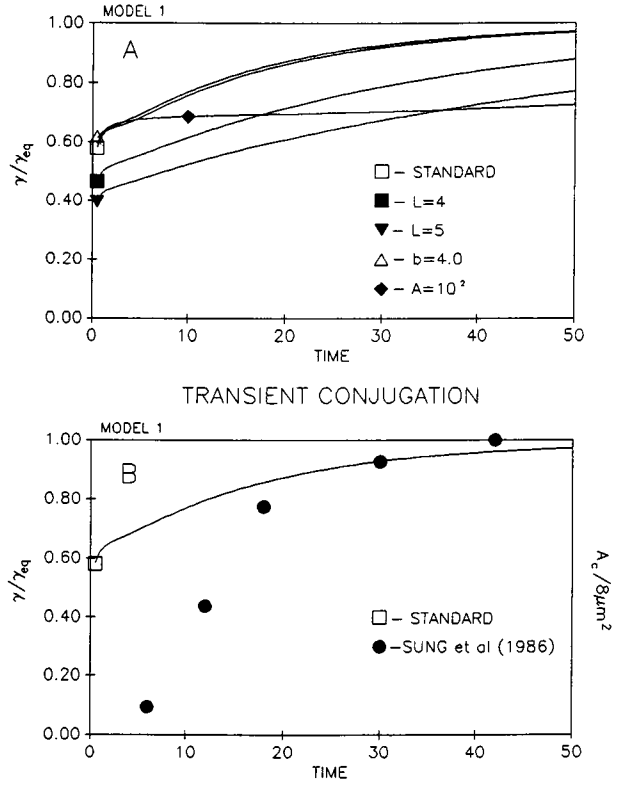

FIGURE 7 The variation of adhesive energy density (γ) with respect to time (T) during transient conjugation for model 1 (mobile M and N). Standard curve corresponds to the parameter values: $A = 1{,}000$, $b = 2.5$, $C = 10$, $d = 1$, and $L = 3$. The other curves in the figure were obtained by changing one of the parameter values at a time. That parameter is indicated in the graph. The circular points shown in Fig. 7 *B* indicate the area of conjugation between F1 and JY measured by Sung et al. (12) at various times during the duration of incubation (see Fig. 1 in [12]). The experimental times were multiplied in *B* by $g_0 = 0.05\ S^{-1}$ to compare data with dimensionless model computations.

mentioned data on F1-JY interaction. This similarity suggests that in lectin-induced red blood cell aggregation, (*a*) the diffusivity of attached bridges may have been restricted by the spectrin network in the membrane, and (*b*) the rate of detachment g is slow. In lectin-induced aggregation unattached bonds represent the specific receptor sites (glycoproteins) on membrane surfaces for lectin binding. Attached bonds are then formed by the attachment of a lectin molecule to one or more receptor sites on opposing sides of the cell surfaces.

4. BONDS WITH MULTIPLE ATTACHED STATES

In previous sections we have assumed a single bond type to be responsible for adhesion. This is a simplification in many cases of specific adhesion. For example, the adhesion between a T-cell (F1) and its target cell (JY) is induced by binding of TCR, CD2, and LFA-1 molecules on the surface of F1 with receptor molecules MHCII, LFA-3, and ICAM-1 on JY (3). Strength of binding of each type of molecule can ideally be studied one at a time by micromanipulation using cytotoxic T-lymphocyte clone where the cell surface contains only the molecule under consideration. It is expected that some of the bonds will be weak and others will be strong. Adhesive energy density measured in micromanipulation (γ) will be due to the cumulative contribution of all these bonds. The kinetic equations show that weak bonds will detach before having the chance to significantly slide towards the region of conjugation during cell separation, so that the increase in γ with the extent of separation of a conjugated F1-JY pair is due to the strongly bound molecule types.

An important feature of lectin-induced red blood cell

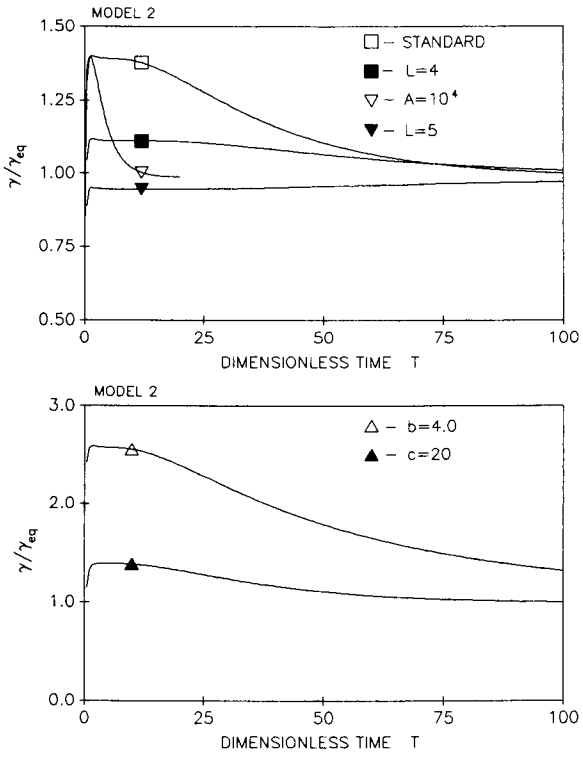

FIGURE 8 The variation of adhesive energy density (γ) with respect to time T during transient conjugation for model 2 (mobile M, immobile N). Standard curve corresponds to the parameter values: $A = 1{,}000$, $b = 2.5$, $c = 10$, $d = 0$, and $L = 3$. The other curves in the figure were obtained by changing the value of one parameter at a time.

aggregation is that during forced separation the peel tension is several orders of magnitude larger than the tension that prevents further conjugation. A possible explanation of this experimental observation may be the existence of at least two attached states for a bond: a weakly attached state (N_w) and a strongly attached state (N_s). The cross-bridge cycle is then defined by the following kinetic scheme:

$$M \underset{g}{\overset{f}{\rightleftharpoons}} N_w \underset{i}{\overset{h}{\rightleftharpoons}} N_s, \tag{16}$$

where f, g, h, and i denote the transition rates and M is the unattached state. In the case of skeletal muscle fibers, N_s would denote the rigor cross-bridge state, whereas N_w corresponds to an actomyosin cross-bridge with bound nucleotide (an ATP hydrolysis product). The transformation from N_w to N_s in muscle fibers occurs by the detachment of the nucleotide. N_s can also be obtained directly from an unattached state in a bathing solution in which no nucleotide is present. In cell–cell adhesion the possible role of energy producing molecules such as ATP on bond cycle has not yet been fully explored (Bell et al. [31]). However, one can think up a possible biochemical scheme in which weakly attached bridges are transformed into strongly attached bridges ($b \to \infty$) as a result of bridge stretching induced by peel tension. Let A_m, A_{nw}, and A_{ns} be the standard free energy of a bond associated with states M, N_w, and N_s. A_{nw} and A_{ns} are assumed to be functions of bond extension in the following form (see Fig. 9):

$$A_{nw} = A_w + (1/2)K_w y^2$$

$$A_{ns} = A_s + (1/2)K_s(y - \delta)^2, \tag{17}$$

where δ, K_w, K_s, A_w, and A_s are constants $(A_m - A_w) > 0$ and $(A_w - A_s) > 0$. The rate functions f, g, h, i satisfy the following equations of detailed balance:

$$(g/f) = \exp\left[-b + \frac{K_w}{2K_bT_b}y^2\right]$$

$$(h/i) = \exp\left[b_1 + \frac{k_w}{2K_bT_b}y^2 - \frac{K_s}{2K_bT_b}(y - \delta)^2\right], \tag{18}$$

where $b = (A_m - A_w)/k_bT$ and $b_1 = (A_w - A_s)/k_bT$. The bond density distribution under equilibrium conditions can then be computed by the following relations:

$$M = (g/f)/[1 + (g/f) + (h/i)]$$

$$N_w = 1/[1 + (g/f) + (h/i)]$$

$$N_s = (h/i)/[1 + (g/f) + (h/i)]. \tag{19}$$

Our computations with parameter values: $b = 2.5$, $b_1 = 5.0$, $(K_w H^2/kT) = 10$, $(K_s H^2/k_bT_b) = 40$, and $\delta = 10$ nm show that at equilibrium, the number of attached bridges (N_w, N_s) decays rapidly towards zero as $y \to \infty$. If the rate of attachment f is small at $y = \delta$, the density of

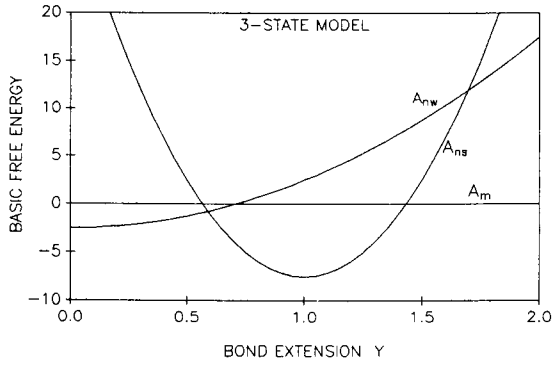

FIGURE 9 The standard free energy distribution as a function of bond extension y for all three states of an adhesive bond ($K_wH^2/K_bT_b = 10$, $K_sH^2/K_bT_b = 40$, $H = 10$ nm, $\delta = 10$ nm, $b = 2.5$, $b_1 = 5.0$).

strongly attached bridges will be negligible during transient conjugation.

Let us now consider a step increase in the extent of peeling (Δ) induced by a hypothetical force system. The equilibrium bond density distribution will then shift right a distance (Δ). According to the rate equations (19), weakly attached bonds will be more likely to transfer to a strongly bound state than detach. Hence, the transients following a stretch will show a significant increase in the number of strongly bound bridges. Since binding affinity is a strong determinant of the macroscopic adhesive energy density, γ will also increase.

A similar situation develops during forced separation of cell pairs. According to the scheme shown in Fig. 9, bonds will be most likely weakly attached in the region of conjugation. However, as these bridges are stretched by the peeling membrane tensions, they will first shift to the strongly attached state where they show increased resistance to detachment. After further stretch, strongly attached bridges transform first to the weakly attached state and then they detach. Hence, during forced separation, a weakly attached bond in the region of conjugation will go through the cycle $N_w \rightarrow N_s \rightarrow N_w \rightarrow M$. The lateral mobility of bonds on the surface of the cell membrane may modify this cycle by retarding the rate of bond detachment. Further theoretical and experimental work is necessary to obtain more quantitative information on possible weakly and strongly attached configurations of bonds that hold the cells together.

5. CONCLUSIONS

In this study we have presented a set of numerical experiments to investigate the transient conjugation between cell pairs. In the computations the region of conjugation was assumed to remain constant. Adhesion equations were presented in one-dimensional form, the only independent space variable being the arc length along the meridional direction. The bimolecular kinetics of bond formation was approximated by unimolecular reactions. The numerical computations presented can be shown to be valid when the number of receptors is significantly larger than the number of coreceptors or vice versa. With this choice it is possible to compare our findings with the kinetic model of adhesion presented by Dembo et al. (17). It is expected that the bimolecular nature of bond formation will be important only at the initial stages of transient conjugation before significant redistribution of adhesion molecules takes place.

In the adhesion model we considered two distinct cases. First we assumed that the lateral diffusivity of receptors did not change when they formed bonds. In the second case we assumed that the attached bond is immobile. It is expected that the lateral mobility of surface molecules of adhesion may decrease after bond formation due to the attachment to cytoskeletal structures.

Significant features of micromanipulation data on specific adhesion may be accounted by a simple model of laterally mobile bonds:

(*a*) The parameters that strongly influence the bond migration during transient conjugation are the diffusion coefficients and geometric factors such as the size and the shape of the cells. For biophysically reasonable parameter values it was shown that bond density distribution for FI-JY conjugation approaches equilibrium within 10 min, the duration used in experiments presented by Sung et al. (12).

(*b*) If the diffusion coefficient for the lateral mobility of attached bridges is set equal to zero in the computations, bonds are predicted to accumulate at the edge of conjugation as a result of migration of unattached bridges into the region of conjugation. This prediction is an agreement with preliminary data on lectin-induced red blood cell aggregation. This suggests that the mobility of glycoproteins bound with lectin may be inhibited by the spectrin network on the undersurface of the red blood cell membrane.

(*c*) The membrane tension that prevents further spreading of conjugation is several order of magnitudes smaller than the peel membrane tension that separates cell pairs in lectin-induced red blood cell aggregation (5, 6). As discussed in the previous section, this may suggest the existence of at least two distinct attached states for bridges linking the two-cell surfaces. In this model bridges first form a weakly attached link. These bridges are then transformed into the strongly attached state at the edge of conjugation due to bond extension (distortion) induced by peel membrane tension.

The specific adhesion model presented here does not take into account the possibility of multiple binding sites. For example, *Helix pomotia* lectin used in red cell aggregation has six binding sites per molecule. This ligand forms a link between two red blood cell surfaces by binding specifically to glycophorins on the cell surface. Hence, it is possible that the receptor sites on the same cell surface can be cross-linked by lectin as well as sites on opposing surfaces. However, clear understanding of simple models of adhesion is a first step in building a method for quantification of biophysical parameters of adhesion from micromanipulation data.

APPENDIX 1

Equations governing the time variation of density distributions of attached and unattached bonds on the surface of a spherical cell can be obtained from Eqs. 2 and 4 by replacing $(\partial/\partial x)$ operator with the gradient operator in spherical coordinates (Bird et al. [30]). In the

following we shall consider the axisymmetric diffusion of mobile bonds into the region of conjugation. In this case m and n are functions of only the meridional angle θ and time t. The equation governing the density of unattached bonds can be written as

$$\frac{\partial m}{\partial t} = \frac{D_{mm}}{R^2 \sin\theta}\frac{\partial}{\partial\theta}\left(\sin\theta\frac{\partial m}{\partial\theta}\right) + g\,n - f\,m, \quad \text{(A1.1)}$$

where R is the radius of the sphere. If the attached bonds (n) are assumed immobile ($D_{nn} = 0$), the equation governing n is rather simple:

$$\frac{\partial n}{\partial t} = f\,m - g\,n. \quad \text{(A1.2)}$$

Otherwise,

$$\frac{\partial n}{\partial t} = \frac{D_{nn}}{R^2}\frac{1}{\sin\theta}\frac{\partial}{\partial\theta}\left(\sin\theta\frac{\partial n}{\partial\theta}\right) f\,m - g\,n + \frac{k_b T_b}{R^2}\frac{1}{\sin\theta}\frac{\partial}{\partial\theta}\left(\sin\theta\,n\,y\frac{\partial y}{\partial\theta}\right). \quad \text{(A1.3)}$$

The total number of attached (nt) and unattached (mt) bonds during transient conjugation can be computed by using the following equations:

$$mt = 2\pi R^2\int_0^\pi m\sin\theta\,d\,\theta,\ nt = 2\pi R^2\int_0^\pi n\sin\theta\,d\theta. \quad \text{(A1.4)}$$

The numerical techniques used for the computations of m and n on the spherical surface of a cell is described in Appendix 2.

APPENDIX 2

The equations governing transient conjugation form a set of nonlinear partial differential equations of the form:

$$U_t = f(X, t, U_x, U_{xx}), \quad \text{(A2.1)}$$

where U denotes the column vector of dependent variables, X is the space variable, t is time, U_t is the partial derivative of U with respect to t, U_x and U_{xx} are, respectively, the first and second order partial derivatives with respect to X. We have used a collocation method in which the space variable X is divided into a finite number of intervals and the dependence of U with respect to X is approximated by using cubic hermit polynomials. These are piecewise cubic polynomials with continuous first derivatives. The partial differential equations (Eq. A2.1) then reduce to a set of ordinary differential equations for determining the time variation of the coefficients of Hermit polynomials. The software package DMOLCH from IMSL Math Library was used for numerical solution of Eq. A2.1. The dimensionless arc length X was discretized at equal increments, $\Delta X = 1$, except at the edge of conjugation and the boundaries. At the edge of conjugation (represented as a quarter circular arc [$0 < X < 5$]) increment in X was 0.1. This increment was increased linearly to the left and right in 10 units of X to the value $\Delta X = 1$. The reason for smaller increments at the edge of conjugation was due to the rapidly changing values of the rate functions in this region. ΔX was set equal to 0.25 at the boundaries for 5 units of arc length and then linearly increased to 1 in a domain of 10 arc lengths. For the standard case shown in Fig. 4, the total number of discrete X values for which M and N were computed was 476. This number increased to 676 when the length of the unconjugated region was expanded from 2 to 4. Our computations showed that the accuracy of solution improved significantly by decreasing the increment in X at the edge of conjugation and at boundaries. The accumulative error in computations is controlled by a tolerance parameter TOL. However, in our case even a more sensitive indicator was the total number of cross-bridges. This number did not vary >1% in all the graphs presented in the paper. We have also checked the solution to see if the boundary conditions on N and M were satisfied. In equations corresponding to model 1 we have chosen M as $U(1)$ and N as $U(2)$. However, the accuracy of the solution near $S = -Z$ (center of conjugation) was not satisfactory when N is set equal to zero as the initial condition. Note that the no flux boundary condition at $S = -Z$ required also that $\partial N/\partial S = 0$. The accuracy increased to satisfactory (tol = 0.001) when we started the computations with the initial condition that N and M rapidly reached equilibrium at time $t = 0$ with $N + M = 1$. This assumption is quite reasonable for the high attachment rates (f/g) used in the computations. Our numerical results indicate that the rise in γ is first due to attachment of bonds already in the region of conjugation and then due to the attachment of additional bridges that moved to the region at a later time.

The computations for model 2 (mobile M, immobile N) were carried out similarly. In this case $U(1) = M$ and $U(2) = M + N$. Initial conditions at $t = 0$ were: $U(1) = 1$, $U(2) = 1$. The boundary conditions were again that $\partial U(1)/\partial X = \partial U(2)/\partial X = 0$ at $S = -Z$ and $S = L$.

I would like to thank Drs. Shu Chien and Yi-der Chen for discussions on specific adhesion. I would also like to thank Mr. John-Erik Conrey for helping with numerical computations and graphics.

This research was supported by National Institutes of Health grant No. R01-GM41460 and National Science Foundation grant No. DCB-8719006.

Received for publication 27 November 1989 and in final form 2 May 1990.

REFERENCES

1. Hynes, R. O. 1987. Integrins: a family of cell surface receptors. *Cell.* 48:549–554.
2. Ruoslahti, E., and M. D. Pierschbacher. 1987. New perspectives in cell adhesion: RGD and integrins. *Science (Wash. DC).* 238:491–497.
3. Springer, T. A., M. L. Dustin, T. K. Kishimoto, and S. D. Marlin. 1987. The lymphocyte function associated LFA-1, CD2 and LFA-3 molecules: cell adhesion receptors of the immune system. *Annu. Rev. Immunol.* 5:223–252.
4. McClay, D. R., and C. A. Ettensohn. 1987. Cell adhesion in morphogenesis. *Annu. Rev. Cell Biol* 3:319–345.
5. Evans, E. A., and K. Baxbaum. 1981. Affinity of red blood cell membrane for particle surfaces measured by the extent of particle encapulation. *Biophys. J.* 34:1–12.
6. Evans, E. A., and A. Leung. 1984. Adhesivity and rigidity of erythrocyte membrane in relation to wheat germ agglutinin in binding. *J. Cell Biol.* 98:1201–1208.
7. McCloskey, M. A., and M. Poo. 1986. Contact-induced redistribution of specific membrane components: local accumulation and development of adhesion. *J. Cell Biol.* 102:2185–2196.
8. Chien, S., and L. A. Sung. 1987. Physiocochemical basis and clinical implications of red cell aggregation. *Clin. Hemorheol.* 7:71–91.
9. Vayo, M., R. Skalak, P. Brunn, S. Usami, and S. Chien. 1987. The role of the surface adhesive energy in shear disaggregation of red cell rouleaux. *Fe. Proc.* 46:1043.

10. Evans, E. A. 1985. Detailed mechanics of membrane–membrane adhesion and separation. I. Continuum of molecular crossbridges, *Biophys. J.* 48:154–183.

11. Evans, E. A. 1985. Detailed mechanics of membrane–membrane adhesion and separation. II. Kinetically trapped molecular cross-bridges. *Biophys. J.* 48:185–192.

12. Sung, K. L. P., L. A. Sung, M. Crimmins, S. J. Burakoff, and S. Chien. Determination of junction acidity of cytotoxic T-cell and target cell. *Science* (*Wash. DC*). 234:1405–1408.

13. Bell, G. I. 1978. Models for the specific adhesion of cells to cells. *Science* (*Wash. DC*). 200:618–627.

14. Bell, G. I., M. Dembo, and P. Bongrand. 1984. Cell–cell adhesion: competition between nonspecific repulsion and specific bonding. *Biophys. J.* 45:1051–1064.

15. Bongrand, P., C. Capo, and R. Depieds. 1982. Physics of cell adhesion. *Prog. Surf. Membr. Sci.* 12:217–285.

16. Dembo, M., and G. I. Bell. 1987. The thermodynamics of cell adhesion. *Curr. Top. Membr. Transp.* 29:71–89.

17. Dembo, M., D. C. Torney, K. Saxman, and D. Hammer. 1988. The reaction limited kinetics of membrane to surface adhesion and detachment. *Proc. R. Soc. Lond. B. Biol. Sci.* 234:55–83.

18. Tozeren, A., K. L. P. Sung, and S. Chien. 1989. Theoretical and experimental studies on cross-bridge migration during cell disaggregation. *Biophys. J.* 55:479–487.

19. Tozeren, A. 1989. Adhesion induced by mobile cross-bridges: steady state peeling of conjugated cell pairs. *J. Theor. Biol.* 140:1–17.

20. Abney, J. R., A. Scalettar, and J. C. Owicki. 1989. Self diffusion of interacting membrane proteins. *Biophys. J.* 55:817–835.

21. Abney, J. R., B. A. Scalettar, and J. C. Owicki. 1989. Mutual diffusion of interacting membrane proteins. *Biophys. J.* 56:315–329.

22. Eisenger, J., and B. I. Halperin. 1986. Effects of spatial variation in membrane diffusibility and solubility on the lateral transport of membrane components. *Biophys. J.* 50:513–521.

23. Small, R. K., M. Blank, R. Ghez, and K. H. Pfenninger. 1984. Components of the plasma membrane of growing axons. II. Diffusion of membrane complexes. *J. Cell Biol.* 98:1434–1443.

24. Singer, S. J., and G. L. Nicolson. 1972. The fluid mosaic model of the structure of cell membranes. *Science* (*Wash. DC*). 175:720–731.

25. Cantor, C. R., and P. R. Schimmel. 1980. Biophysical Chemistry. II. Techniques for the Study of Biological Structure and Function. W. H. Freeman and Co., San Francisco, CA. 532 pp.

26. Huxley, A. F. 1957. Muscle structure and the theories of contraction. *Prog. Biophys. Biophys. Chem.* 7:255–318.

27. Hill, T. L. 1974. Theoretical formalism for the sliding filament model of contraction of striated muscle, Part 1. *Prog. Biophys. Mol. Biol.* 28:267–340.

28. Tozeren, A. 1987. The influence of doubly attached cross-bridges on the mechanical behavior of skeletal muscle fibers under equilibrium conditions. *Biophys. J.* 52:901–906.

29. Tozeren, A., and M. Schoenberg. 1986. The effect of cross-bridge clustering and head–head competition on the mechanical response of skeletal muscle fibers under equilibrium conditions. *Biophys. J.* 50:875–884,

30. Bird, R. B., W. E. Stewart, and N. Lightfoot. 1960. Transport Phenomena. John Wiley & Sons, Inc., New York. 780 pp.